ACS OMEGA

http://pubs.acs.org/journal/acsodf

Article

Conversion of Harmful Fly Ash Residue to Zeolites: Innovative Processes Focusing on Maximum Activation, Extraction, and Utilization of Aluminosilicate

Huidong Liu*

Cite This: *ACS Omega* 2022, 7, 20347−20356

Read Online

ACCESS | Metrics & More | Article Recommendations

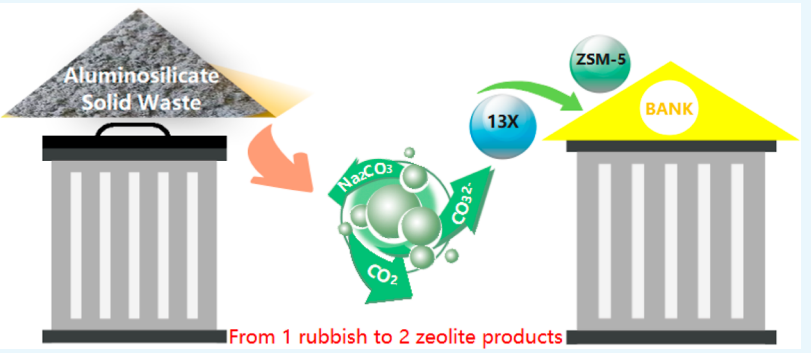

ABSTRACT: Reuse of the solid residue from coal fly ash alumina extraction (FAAE) by acid leaching is problematic. Conversion of this solid residue into aluminum-rich zeolite (13X) and silicon-rich zeolite (ZSM-5) was investigated in this research. The FAAE residue was activated by alkali roasting with Na_2CO_3 powder (110% mass fraction) at 890 °C for 60 min. Silicon and aluminum were mainly present as two mineral phases, Na_2SiO_3 and $NaAlSiO_4$, respectively, in the product obtained after roasting. The roasted product was dissolved in water (liquid/solid ratio of 2) after 20 min at 100 °C. The water-leaching liquor was investigated for total conversion to aluminosilicate zeolites without external aluminum or silicon addition. Hydrothermal synthesis of aluminum-rich zeolite 13X was successful after fine tuning of the conditions, although the filtrate had an unusually high SiO_2/Al_2O_3 molar ratio. Production of 13X consumed a large amount of aluminum, which increased the Si/Al ratio to a level suitable for synthesis of ZSM-5. The synthesis of ZSM-5 from the mother liquor of 13X was proved feasible. The FAAE residue was transformed into high-value zeolite products by nearly 100%. Additionally, the tail liquid of this process, mainly containing Na_2CO_3, was completely recycled. This process could be used to realize high-efficiency and high-value utilization of similar aluminosilicate solid wastes.

1. INTRODUCTION

Large-scale and efficient disposal of fly ash is problematic in China. To meet reduction targets for solid waste, the China Energy Group, which is the world's largest coal and thermal power producer, has been investigating extraction of alumina from fly ash with a high alumina content at Zhungeer (Inner Mongolia, China).[1,2] Leaching of this fly ash with hydrochloric acid produces metallurgical-grade alumina.[3−5] By-products such as lithium, gallium, and other rare metals could also be recovered from the fly ash in the near future.[6−9] However, the secondary solid waste created after alumina extraction from the fly ash is difficult to dispose of. According to relevant policies in China,[10] alumina production plants that use fly ash as raw material should find uses for more than 96% of the waste. Insufficient use or disposal of the solid residue obtained after alumina extraction severely limits the development of alumina-rich fly ash as a resource. Thus, development of high-efficiency and high-value reuse technologies for the solid residue obtained after alumina extraction is of practical significance to relieve environmental pressures and promote industrial utilization of alumina-rich fly ash.

The solid residue obtained after alumina extraction is highly enriched in silicon (SiO_2 mass fraction of 60−80%, ash basis). Previous research on the solid residue obtained after alumina extraction has mainly focused on the production of silica-based materials such as autoclaved bricks, active calcium silicate, glass−ceramics, silicon carbide, and rubber fillers.[11−16] The

Received: April 17, 2022
Accepted: May 17, 2022
Published: May 27, 2022

Table 1. Elemental Composition (%) of the FAAE Residue and Its Desilication Product[a]

	SiO_2	Al_2O_3	P_2O_5	SO_3	K_2O	CaO	TiO_2	Fe_2O_3	ZrO_2	Na_2O
FAAE residue	78.7	13.4	0.14	0.35	0.16	0.37	5.2	0.45	0.29	bdl
desilication product	23.2	56.7	0.1	0.67	0.12	0.95	11.7	1.71	0.48	3.44

[a]bdl: below the minimum detection limit.

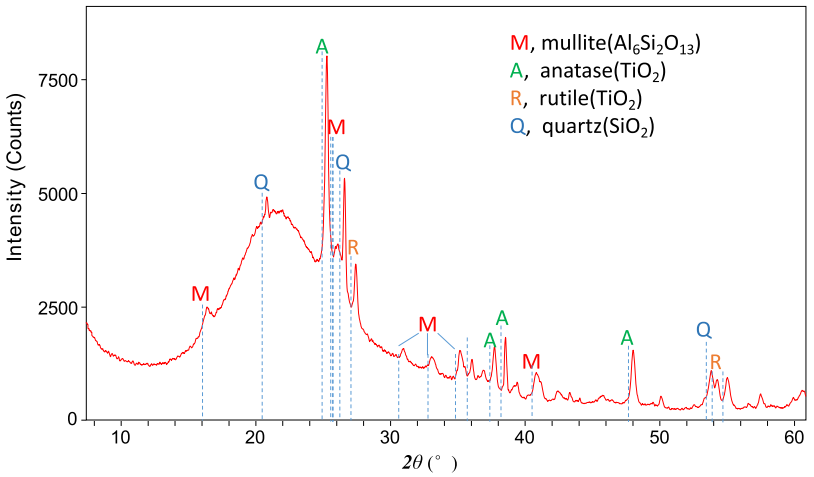

Figure 1. Mineral phase composition of the FAAE residue by XRD qualitative analysis.

aluminum (Al_2O_3 mass fraction of 10−30%, ash basis) still left in the solid residue has not been fully utilized.

The most commonly used zeolites are artificial aluminosilicate minerals with uniform pore structures. Because of their high adsorption capacities, strong thermal stabilities, and other parameters, zeolites have been widely applied in catalytic cracking,[17−19] adsorption and separation,[20,21] ion exchange,[22,23] and many other important functions with a considerable economic value.[24] The solid residue obtained after alumina extraction has a chemical composition suitable for preparation of zeolites 4A, 13X, ZSM-5, and other aluminosilicate zeolites. These materials provide a potential utilization approach for the solid residue obtained after alumina extraction, the original fly ash, and similar solid wastes.

Zeolites are commonly synthesized from fly ash using either the direct (or one-step) method or the indirect method.[25,26] For the direct method, fly ash obtained after roasting activation or without any treatment is hydrothermally crystallized for zeolite production. Dissolution of the fly ash and crystallization of zeolite proceed simultaneously. It is thought that zeolite crystals grow around the undissolved fly ash particles, which hinders further dissolution of the fly ash and means that pure zeolite products are not obtained. In the indirect method,[27−29] the aluminum source or the silicon source is separated from the fly ash by acid or alkali leaching. Then, a gel with a specific chemical composition obtained by the addition of a silicon source (e.g., Na_2SiO_3) or an aluminum source (e.g., $AlCl_3$) solution is prepared. Finally, the gel is used for hydrothermal synthesis of the target zeolite. This indirect synthesis guarantees the purity of the zeolite product but is a complicated process that results in excessive consumption of energy and acid or alkali.

This work aims to overcome current issues with the direct and indirect methods and simultaneously promote the conversion rate as well as the product value of the fly ash alumina extraction (FAAE) residue. An innovative conversion process involving alkali roasting, water leaching at atmospheric pressure and low temperature, and sequential synthesis of zeolite 13X and ZSM-5 was proposed. Alkali roasting helps fully break up the crystal structures of mullite and quartz and release Si and Al. After water leaching, the liquid phase containing both Si and Al was then used as a combined Si- and Al-source for syntheses of two types of zeolites. It is hoped that this work could provide some common reference for the reuse of similar aluminosilicate solid wastes in the future.

2. MATERIALS AND METHODS

2.1. Materials. The composition of the FAAE residue was SiO_2 78.7%, Al_2O_3 13.4%, and TiO_2 5.2% (Table 1). X-ray diffraction (XRD) analysis (Figure 1) indicated that the solid residue contained mullite ($3Al_2O_3−SiO_2$), quartz (SiO_2), anatase (TiO_2), and rutile (TiO_2). The main carrier minerals for Al_2O_3 and SiO_2 are mullite and quartz, and the main carrier minerals for TiO_2 are anatase and rutile. These minerals with quite stable crystal structures would exhibit fairly low reactivity in the process of activation and conversion of solid waste disposal or reuse. SiO_2 is found more in amorphous glass. The percentage of amorphous silica in the FAAE residue can be characterized using the integrated intensity of the diffuse peak existing in the 2θ = 15−35° section of the XRD spectral line (Figure 1). Previous studies in our laboratory have shown that amorphous silica in the FAAE residue can be easily extracted using 6 mol/L of NaOH at 95 °C and atmospheric pressure for 0.5−1.0 h without pre-roasting; the total mass of the FAAE residue could be reduced by approximately 70% after desilication.[30,31]

However, its secondary residue (entry 2, Table 1) after desilication treatment becomes more difficult to undertake further conversion and reuse because of its poorer reactivity. It is obvious that more drastic activation methods are necessary.

SiO_2 and Al_2O_3 account for more than 90% of the FAAE residue by mass, and utilization of them for preparation of Si−O−Al-based zeolites will facilitate fly ash disposal of volume reduction and value promotion. Iron, calcium, and other metal ions usually affect the structure and performance of zeolites.

https://doi.org/10.1021/acsomega.2c02388
ACS Omega 2022, 7, 20347−20356

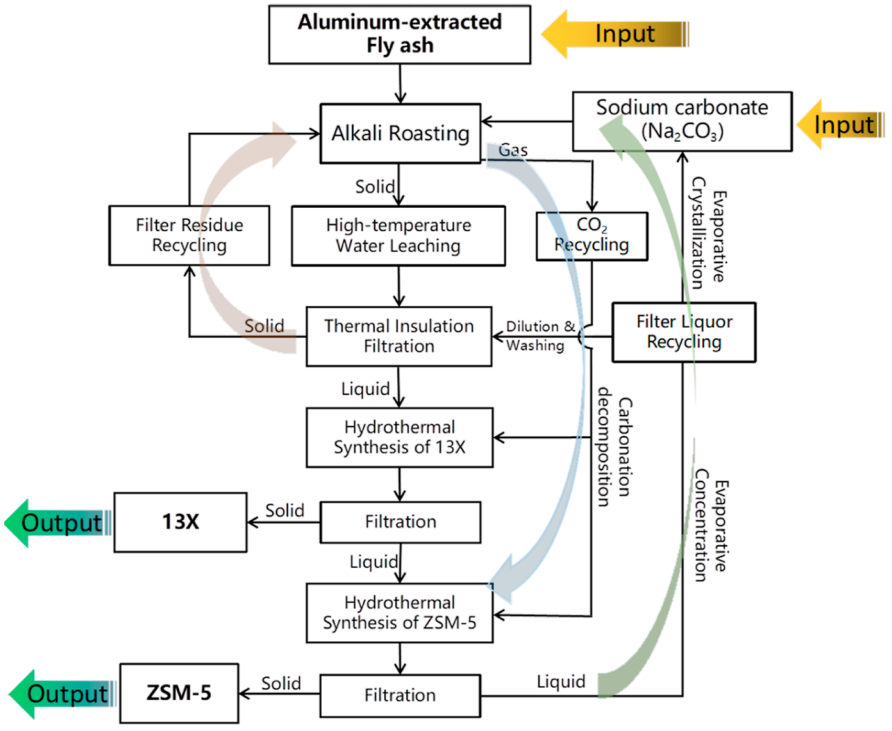

Figure 2. Technical flow chart for conversion of the FAAE residue to zeolites with maximum waste recycling of the solid, liquid, and gas.

Benefiting from the acid-leaching treatment of FAAE, the solid residue of FAAE is more suitable for the synthesis of aluminosilicate zeolites than the original fly ash as iron, calcium, and other acid-soluble harmful components were removed along with aluminum in advance.

2.2. Methods. A four-step process was designed for simultaneous synthesis of zeolites 13X and ZSM-5 from the FAAE residue (Figure 2).

The first step was alkali roasting. In this step, the FAAE residue was mixed with Na_2CO_3 (110−130% mass fraction) and roasted at 830−910 °C for 60−90 min to effectively activate silicon and aluminum. Molten Na_2CO_3, which may contain some Na_2O (a decomposition product of Na_2CO_3), will destroy the structure of aluminosilicate crystals and form new water-soluble substances. This step is the key to the decomposition and reuse of the aluminosilicate solid waste. In future large-scale production, CO_2 in the roasting tail gas can be collected and used for the subsequent CO_2-bubbling process.

The second step was water leaching. In this step, the alkali roasting product was crushed to less than 200 mesh. This was followed by dry magnetic separation of the iron. A one-step water leaching process was then used to dissolve active silicon and aluminum from the roasted solid residue. The leaching temperature (T_1) was 60−100 °C, the liquid to solid ratio (LSR) was 2−20 (mL/g), and the leaching time (t) was 20−120 min. The mixture was then filtered while still warm (T_2 = 20−75 °C) to separate the Si- and Al-rich aqueous phase from the solid residue. The aqueous phase was used as the raw material for zeolite synthesis. The solid residue from warm filtration was recycled back into the alkali roasting step, which minimized the production of secondary solid waste. Saturated Na_2CO_3 solution from the fourth step was used to dilute and wash the product from the water leaching process.

The third step was synthesis of zeolite 13X. For this step, 100 mL of water was added to approximately 400 mL of the Si- and Al-rich water-leaching liquor from the second step of preliminary hydrolysis. Then, CO_2 gas was bubbled into the system, and the mixture was hydrolyzed further to a certain pH value to prepare the precursor for synthesis of 13X. The zeolite was then synthesized in a polytetrafluoroethylene reactor at 90−110 °C for 15−30 h. The mother liquor obtained after removal of 13X by filtration was retained for subsequent synthesis of ZSM-5.

The fourth step was synthesis of zeolite ZSM-5. For this step, the mother liquor of 13X was further hydrolyzed by bubbling CO_2 gas again to a lower pH. Next, tetrapropylammonium hydroxide (TPOH) was introduced into the system as a template to prepare the precursor for ZSM-5. The ZSM-5 precursor was then transferred into a polytetrafluoroethylene reactor and crystallized under hydrothermal treatment (140−190 °C) for 24−72 h. The solid crystallization product was then filtered and washed using excess water to thoroughly remove Na_2CO_3 from the filter cake. After filtering and washing, the solid product was dried at 120 °C for more than 4 h and then roasted at 550 °C for 4 h to remove the organic template. The roasting product was pure sodium-type ZSM-5. The mother liquor of ZSM-5 contained mainly Na_2CO_3 and a small amount of silicon and aluminum. The Na_2CO_3 from the liquor was recycled back into steps 1 and 2 after evaporation, concentration, and crystallization. This minimized the volume of the waste liquid created in this step.

2.3. Analysis. X-ray fluorescence spectrometry (XRF; ZSX Primus, Rigaku, Tokyo, Japan) was used to quantitatively analyze the chemical elements in the solid residue obtained after alumina extraction, the intermediates, and the zeolite products. The instrument used contained a 4 kW X-ray tube with an ultra-thin 30 μm Rh window and was equipped with an 8-crystal converter (LiF200, PET, RX-61/45/35/25, Ge, and LiF220). Data were obtained for the elements from boron to uranium, and the measurement accuracy was at the parts per million level.

https://doi.org/10.1021/acsomega.2c02388
ACS Omega 2022, 7, 20347−20356

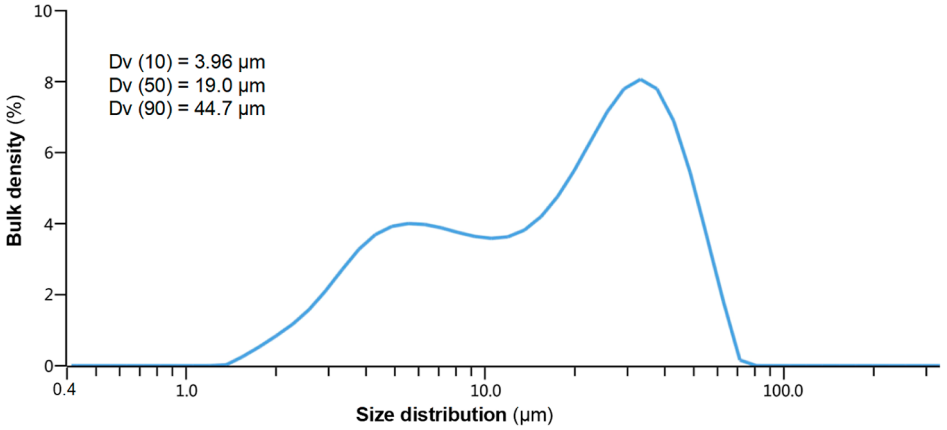

Figure 3. Particular size distribution of the FAAE residue.

XRD analysis of all samples was performed using a powder diffractometer (D8 Advance, Bruker, Germany) equipped with a ceramic X-ray tube (40 kV, 40 mA), a Cu Kα radiation source, and an energy resolution of <9%. All samples were scanned within a 2θ interval of 4−70° using a step size of 0.01°. EVA and TOPAS software (Bruker) were applied to the data to identify the mineral phases in the samples.

A field-emission scanning electron microscope (SEM; Nova NanoSEM, FEI, USA) was used in conjunction with an energy-dispersive X-ray spectrometer (X-man 50, Oxford Instruments, UK) to obtain information about the micromorphologies and elemental compositions of the zeolites synthesized in this study.

As for the determination of the chemical composition of the precursor liquor used for the zeolites syntheses, the content of Na, Si, Al, and other elements was determined by ICP-AES (SPECTRO ARCOS, Spectro, Germany), and the concentration of the CO_3^{2-} ion was determined using the ion-selective electrode (PXS-CO2, Hangzhou Qiwei Instrument Co., LTD, China). The mass of H_2O was obtained by subtracting the total mass of measured ions from the total mass of the solution. Then, all the mass concentrations were converted to molarities to characterize the chemical composition of the precursor.

A laser particle size analyzer (Mastersizer 3000, Malvern Panalytical, UK) was used to analyze the particle size distribution of raw materials and products. The N_2 adsorption−desorption isothermal curves were obtained at 77 K (3-FLEX, Micromeritics, USA). The specific surface area was determined via the Brunauer−Emmett−Teller (BET) equation.

3. RESULTS AND DISCUSSION

3.1. Mineral Phase Transition during Alkali Roasting and Activating Effect. Dv(X) was defined as the diameter at which X % (by volume) of the particles have a diameter less than that value. The particle size property of powder sample can be basically obtained commonly by fetching the values of Dv(10), Dv(50), and Dv(90). The FAAE residue particles have good fineness (Dv(90) = 44.7 μm, Figure 3), which is conducive to their subsequent activation or transformation reaction. No individual mineral particles (e.g. mullite, anatase, or quartz) were found under the SEM. Irregular particles adhering to each other (Figure 4) indicate that physical separation methods would be ineffective in extracting any single component.

Alkali (adding NaOH or Na_2CO_3) roasting is an effective method to decompose or activate aluminosilicate minerals.[32−34] In the subsequent dissolution and extraction process, separating

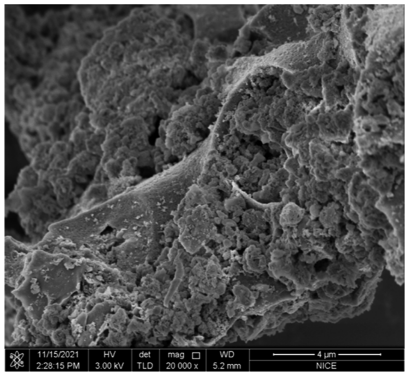

Figure 4. SEM image of the raw FAAE residue.

aluminum by acid-leaching and silicon by alkali-leaching, respectively, is a common approach.[35,36] The natural consequences of using both acids and alkalis in the same system involve increased acid and alkali losses, more complex operation procedures, and an extra investment in acid- and alkali-proof equipment and pipelines. Silica and alumina could react with Na_2CO_3 and be transformed completely into water-soluble Na_2SiO_3 and alkali-soluble $NaAlSiO_4$[37] under proper roasting conditions. It seems feasible to complete roasting (aluminosilicate activation), leaching (Si & Al extraction), and utilization (zeolites hydrothermal syntheses) of aluminosilicate waste under a single alkali reaction system. Maximum conversion and use of the FAAE residue at the lowest cost of energy and materials would be achievable.

The effects of addition of sodium carbonate, the roasting temperature, and the roasting time on the composition of the alkali roasting product were investigated to optimize the alkali roasting conditions for subsequent Si and Al dissolution and zeolite syntheses. The XRD results (Figure 5) indicated that the alkali roasting products all contained Na_2SiO_3, sodium silicoaluminate, amorphous aluminosilicate glass, and Na_2CO_3 in different proportions.

As we all know, mineral phase content is positively correlated with the intensity of the diffraction peak. The original diffraction spectrums of alkali roasting products obtained under the same test conditions were stacked and compared in XRD analysis software (e.g., JADE). By observing the intensity (height) variation of the diffraction peaks of each mineral phase with different roasting conditions, their influence on the relative proportion of each phase (including the amorphous alumi-

https://doi.org/10.1021/acsomega.2c02388
ACS Omega 2022, 7, 20347−20356

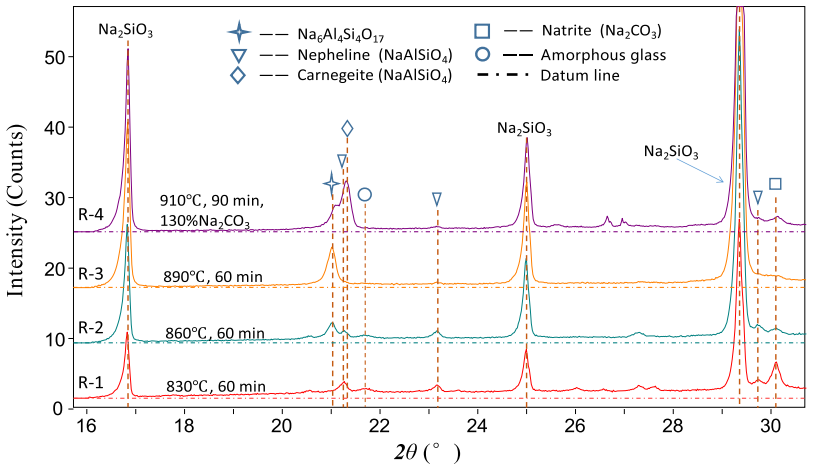

Figure 5. Mineral phase transition of alkali (110% mass fraction of Na_2CO_3)-roasted FAAE residue under various conditions.

nosilicate glass) can be qualitatively predicted without the need to calculate their exact containing values.

As the roasting temperature increased, the proportions of Na_2SiO_3 and $NaAlSiO_4$ increased, and the proportion of amorphous glass decreased. Transformation of the mineral phases of sodium silicoaluminate occurred as follows: nepheline ($NaAlSiO_4$, 830 °C) → $Na_6Al_4Si_4O_{17}$ (860−890 °C) → carnegeite ($NaAlSiO_4$, 910 °C).

Sodium silicoaluminate in nepheline and carnegeite, amorphous Si and Al, and Na_2CO_3 in the nitrite phase showed poor solubility in the water leaching process and were components of the solid residue obtained after filtration. Therefore, the proportions of nepheline, carnegeite, natrite, and glass should be limited by controlling the roasting conditions. In consideration of the activation effect and the energy cost, a 110% mass fraction of Na_2CO_3, 890 °C, and 60 min were selected as the optimum alkali roasting conditions. The mass fraction of the alkali roasting product compared with the FAAE residue was 156%.

3.2. Optimization of Conditions for Water Leaching of Silicon and Aluminum. Obviously, the leaching rate (LR) of Si and Al is expected to be as high as possible. The LR was calculated as follows

$$\mathrm{LR} = (1 - M_1)/M_0 \times 100\% \quad (1)$$

where M_1 is the mass (dry basis) of the solid residue obtained after water leaching, and M_0 is the mass (dry basis) of the original mass of the FAAE residue used for alkali roasting.

In a desired state, Si and Al were dissolved in NaOH solution and made to coexist in the aqueous phase as sodium silicate and sodium aluminate. Then, the extraction, separation, and reuse of Si and Al would be quite easy. However, actually, the alkali leaching conditions of Si and Al partially overlap with those of the hydrothermal syntheses of zeolites; Si and Al in the alkali hydrothermal environment tend to combine with Na to form sodalite ($Na_8Al_6Si_6O_{24}(OH)_2$) precipitation.[38−40] Zeng et al. (2007)[37] adopted a two-step dissolution strategy (water-leaching for Na_2SiO_3 and NaOH-leaching for $NaAlSiO_4$) to overcome this common issue. Its LR value after two-step dissolution was estimated to be less than 50%, nevertheless. In this study, a single water-leaching procedure was executed to co-extract Si and Al to further simplify the operation and improve the extraction efficiency of Si and Al.

Warm-keeping filtration was first found to be necessary. The dissolution product visibly became sticky when the temperature dropped during the filtration process, resulting in a significant decrease in the LR of Si and Al (entry 1 vs 2, Table 2). Considering the actual operating conditions, T_2 = 75 °C was selected as the feasible filtration temperature.

Table 2. Dissolution Conditions and the Leaching Rates of the Alkali-Roasted FAAE Residue

test no.	liquid to solid ratio LSR (mL/g)	leaching temp. T_1 (°C)	leaching time t (min)	filtration temp. T_2 (°C)	wash agent	leaching rate LR (%)
1	20	100	30	20	none	40.3
2	20	100	30	75		63.0
3	20	100	20	75	water	67.6
4	10	100	20	75		62.4
5	10	100	30	75		59.5
6	10	100	20	75		75.2
7	5	100	20	75	saturated Na_2CO_3 solution	89.7
8	2	100	20	75		93.2

By comparing test no. 4 and no. 5 in Table 2, increasing the leaching time would not increase the LR, which should be attributed to the excessive formation of zeolites (e.g., sodalite) under high alkalinity conditions.

The essence of water leaching is still alkali leaching. The alkalinity may come from the residual Na_2O or Na_2CO_3 or the hydrolysis of sodium (alumino)silicate in the roasted product of the FAAE residue

$$Na_2SiO_3 + H_2O \rightleftharpoons NaOH + SiO_2 - nH_2O\downarrow \quad (2)$$

$$NaAlSiO_4 + H_2O \rightleftharpoons NaOH + SiO_2 - nH_2O \downarrow + Al(OH)_3\downarrow \quad (3)$$

The possible presence of hydrolysis products (SiO_2-nH_2O or/and $Al(OH)_3$) of sodium (alumino)silicate was believed to be another key factor causing filtration difficulty and a decrease in LR. In general, hydrolysis will be intensified by a temperature increase. A low liquid−solid ratio scheme was adopted to inhibit the hydrolysis reaction across the process of high-temperature (T_1 = 100 °C) dissolution. With less H_2O and more Na, the

https://doi.org/10.1021/acsomega.2c02388
ACS Omega 2022, 7, 20347−20356

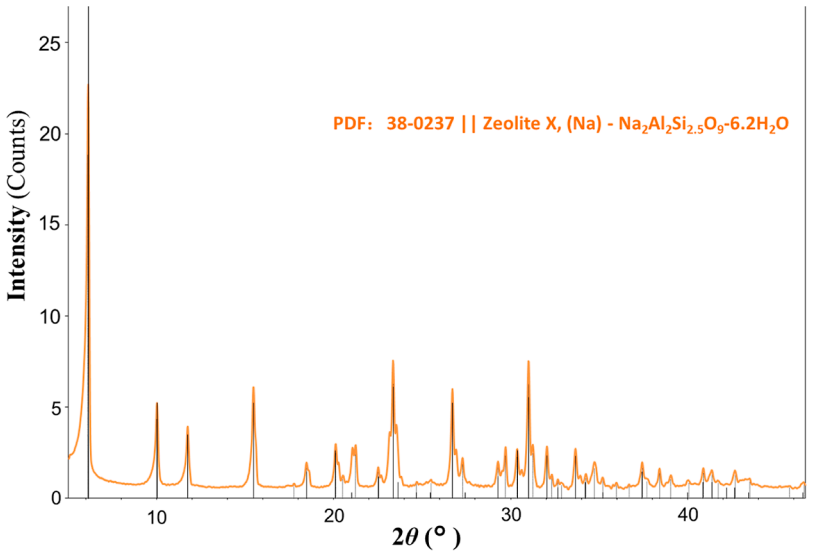

Figure 6. XRD spectrum of zeolite 13X prepared using the water leaching liquor of the alkali-roasted FAAE residue.

chemical eqs 2 and 3 will move to the left side. It is seen (Table 2) that the LR showed an obvious trend of overall rise, while the LSR decreased from 20 to 2 mL/g. When LSR < 2, the roasted sample powder cannot be fully wetted and the dissolution reaction is hard to continue.

Washing the filter cake for removing the attached soluble Si and Al was also found necessary (entry 2 vs 3, Table 2), especially for the tests with lower LSR conditions. However, using hot or cold water as the wash agent led to hydrolysis reaction again. Saturated Na_2CO_3 solution recovered from the end of this process was used as a diluent and washing agent, in view that a mass of Na^+ introduced by Na_2CO_3 would also weaken the hydrolysis. Moreover, the highest LR value of the alkali-roasted FAAE residue reached LR = 93.2% (entry 8, Table 2).

The optimized parameters for water dissolution of the alkali-roasted product were finally determined as (T_1 = 100 °C, t = 20 min, T_2 = 75 °C, LSR = 2−5, using saturated Na_2CO_3 solution as the diluent and washing agent). Under this optimal condition, around 90 wt.% of the FAAE residue can be dissolved and separated for further use. The secondary residue was still dominant with silica and alumina and was sent back for the alkali roasting procedure.

3.3. Co-Production of Zeolites 13X and ZSM-5. The Si- and Al-rich filter liquor collected from Section 3.2 with a molar composition of $SiO_2/Al_2O_3/Na_2O/CO_3^{2-}/H_2O$ = 12:1:13:3.5:40 was taken as the only Si−Al source to synthesize zeolite 13X and ZSM-5.

The theoretical chemical composition of zeolite 13X is $Na_2O{\cdot}Al_2O_3$ (2.8 ± 0.2)SiO_2 (6−7)H_2O. Zeolite ZSM-5 is a typical high-silica zeolite and commonly has a silica/alumina molar ratio (SAR) greater than 30. The SAR value of the filter liquor (SAR = 12) was between that of low-Si zeolite 13X (SAR = 2.6−3.0) and high-Si zeolite ZSM-5 (SAR >30). Adding an external Al-source or Si-source, respectively, to adjust the liquor SAR down or upward for synthesis of 13X or ZSM-5, is the most common thought. However, it is obviously unfavorable in terms of reducing the amount of solid waste.

Assuming that the low-Si zeolite 13X can be directly synthesized with the filter liquor, the mother liquid of 13X will have a higher SAR value suitable for the synthesis of ZSM-5 because most of the Al was consumed by 13X. In this way, the Si and Al in the filter liquor will be converted and utilized with maximum efficiency.

3.3.1. Hydrothermal Synthesis of Zeolite 13X. First, CO_2 gas was used to neutralize the too-high alkalinity of filter liquor to an appropriate pH to prepare the precursor gel for synthesis of 13X. The use of CO_2 gas instead of traditional alkalinity regulators, such as HCl or H_2SO_4 solutions, made recycling of CO_2 and Na_2CO_3 in the overall process possible and avoided corrosion of the equipment by strong acids. Additionally, production of the greenhouse gas CO_2 and highly saline waste water (NaCl or Na_2SO_4) was minimized. Thus, the process was environmentally friendly.

In conventional hydrothermal zeolite syntheses, alkalinity is usually characterized and controlled by two static parameters: Na_2O/SiO_2 and H_2O/SiO_2.[41−43] The levels of these parameters are fixed at the point at which the materials are added. In this study, a single parameter (pH) was investigated for replacing Na_2O/SiO_2 and H_2O/SiO_2 in the 13X and ZSM-5 syntheses. The upper limit of the SiO_2/Al_2O_3 molar ratio for precursors of pure 13X syntheses ever reported has not exceeded 5.4.[44,45] This was the first attempt to synthesize 13X in this ultra-high silicon (SAR = 12) environment.

The experimental results indicated that the pH of the precursor gel had a direct effect on the hydrothermal synthesis of zeolite 13X in this ultra-high silicon system. Precise regulation of the gel pH between 12.9 and 13.6 gave pure 13X crystals (SAR = 2.32, energy dispersive X-ray spectroscopy data) with diameters of less than 15 μm (Figures 6 and 7A) under conventional hydrothermal crystallization conditions (90−110 °C for 15−30 h).

3.3.2. Hydrothermal Synthesis of Zeolite ZSM-5. Recovery and recycling of zeolite mother liquor for the next round of synthesis of the same zeolite are commonly used to induce crystallization and reduce the usage of the template.[46,47] In this study, mother liquor of 13X was used as the material for another kind of zeolite, ZSM-5. This is the major novelty of this work.

Crystallization of 13X consumed excessive Al and Na as expected. The SAR of the mother liquor of 13X increased to 32, and the system alkalinity decreased to approximately pH 12. These values were closer to the ideal conditions for ZSM-5

https://doi.org/10.1021/acsomega.2c02388
ACS Omega 2022, 7, 20347−20356

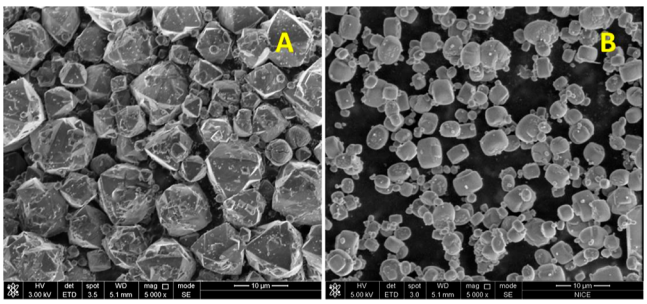

Figure 7. SEM images of zeolites synthesized from the FAAE residue. (A) 13X synthesized at 100 °C for 24 h using the water-leaching liquor of the alkali-roasted FAAE residue. (B) ZSM-5 synthesized at 180 °C for 24 h in the presence of the template polytetrafluoroethylene using the mother liquor of 13X.

synthesis. However, even so, co-crystallization of ZSM-5 and mordenite was found to happen easily, with this SAR level still being relatively low. Impurities of zeolite NaP or analcime were detected when ZSM-5 was directly synthesized under this system alkalinity.

CO_2 was again used to adjust the system alkalinity and also to prepare the precursor of ZSM-5. When the pH was further adjusted to 10.5 by carbonation, pure ZSM-5 crystals (SAR = 24.3, energy dispersive X-ray spectroscopy data) with a diameter size of less than 6.5 μm (Figures 7B and 8) were synthesized in the presence of a template or a seed. The mother liquor of ZSM-5 that mainly contained Na_2CO_3 with trace quantities of silicon and aluminum was recovered to make wash agents (saturated Na_2CO_3 solution) and roasting aids (powder Na_2CO_3).

3.3.3. Further Characterization of Synthesized Zeolites from the FAAE Residue. As shown in Figure 9, particles of zeolite 13X have an ideal normal distribution and good fineness (Dv(90) = 10.1 μm). The particle size distribution of ZSM-5 is bimodal, indicating the presence of a certain proportion of submicron particles (Figure 10).

The specific surface area and pore characteristics of both two zeolites are at normal levels (Table 3). More in-depth characterization of the two zeolites synthesized will be displayed combined with the specific applications in the future.

Metal ions (Ca, Fe, Ti, etc.) other than Si, Al, and Na have positive or negative effects on the adsorption or catalytic performance of zeolites, sometimes significantly. The elemental composition of the synthesized zeolites was analyzed by XRF. The results showed that there was only a trace amount of TiO_2, Fe_2O_3, and others in the two zeolite products (Table 4). This means that the elements Ti or Fe, which may be activated synchronously in the process of alkali roasting, mostly enter into the filter residue of water leaching. After several "roasting-leaching" cycles, Ti with a high economic value will be enriched in the solid phase, from which the recovery of titanium resources may become an unanticipated earning created by this work.

Certain amounts of carbon were detected in both the zeolite products (Table 4), although the occurrence state of carbon is unknown for now. Carbon played an important role in the whole process of decomposition, transformation, and utilization of the solid residue. There have been few reports of the use of CO_2 alone for adjusting and controlling system alkalinity of the hydrothermal syntheses of zeolites in a carbonate (CO_3^{2-}) environment. However, it has been shown that CO_3^{2-} can effectively improve the degree of silica condensation in alkaline media and promote the crystallization of zeolites with Mobil-5 structures (typically, ZSM-5).[48,49] The detailed impact of the CO_3^{2-} environment on the zeolite pore structure and the zeolite acidic and catalytic performance deserves expanded research as this link is of importance for constructing the complete circulation of Na_2CO_3−CO_2−CO_3^{2-} and thus for the full conversion and use of aluminosilicate wastes. The focus on carbon cycling in inorganic chemical processes also has positive environmental implications.

4. CONCLUSIONS

The FAAE residue can be fully activated by alkali roasting with Na_2CO_3 (110% mass fraction) at 890 °C for 60 min. The product from roasting contains silicon and aluminum in the form of Na_2SiO_3 and $NaAlSiO_4$. These minerals dissolve in water after 20 min at 100 °C when the liquid/solid ratio is 2−5. After optimization of the process, the LR of the alkali-roasted FAAE residue reached 90%.

A combined processing strategy was effective for full utilization of the silicon and aluminum in the water leaching liquor of the alkali-roasted FAAE residue. First, the Si- and Al-rich liquor was used to produce low-Si zeolite 13X. After optimization of the hydrothermal conditions for this process, the method was successful even though the SAR was much higher than that conventionally used in 13X synthesis. As expected,

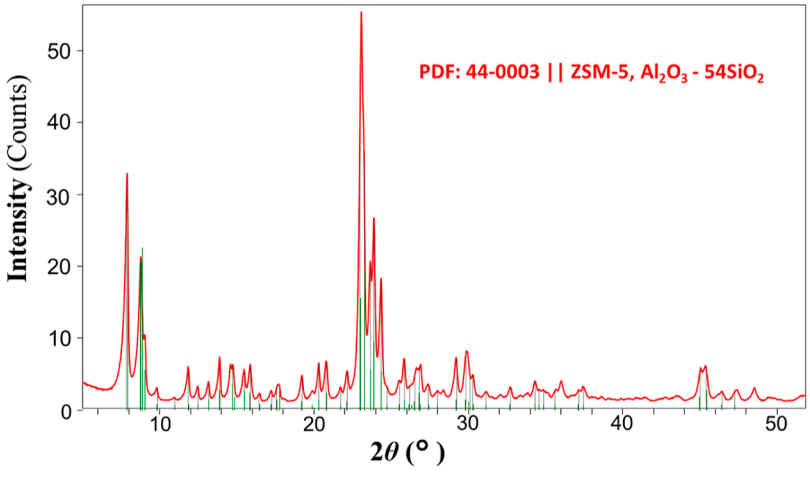

Figure 8. XRD spectrum of the zeolite ZSM-5 synthesized from the mother liquor of 13X.

https://doi.org/10.1021/acsomega.2c02388
ACS Omega 2022, 7, 20347−20356

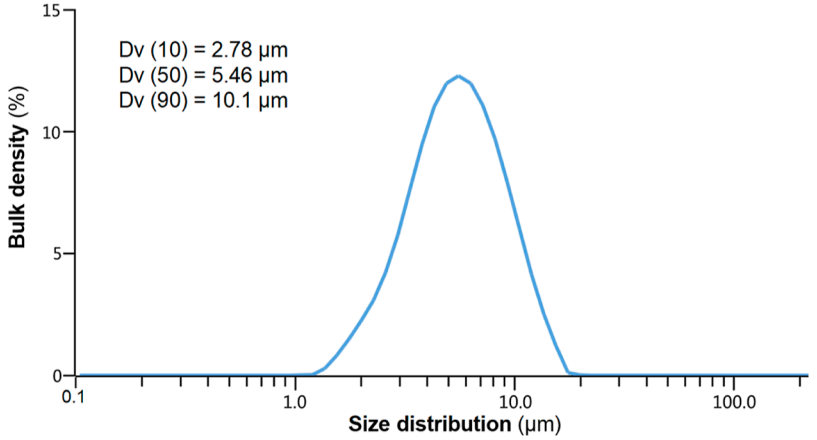

Figure 9. Particular size distribution of the zeolite 13X synthesized from the FAAE residue.

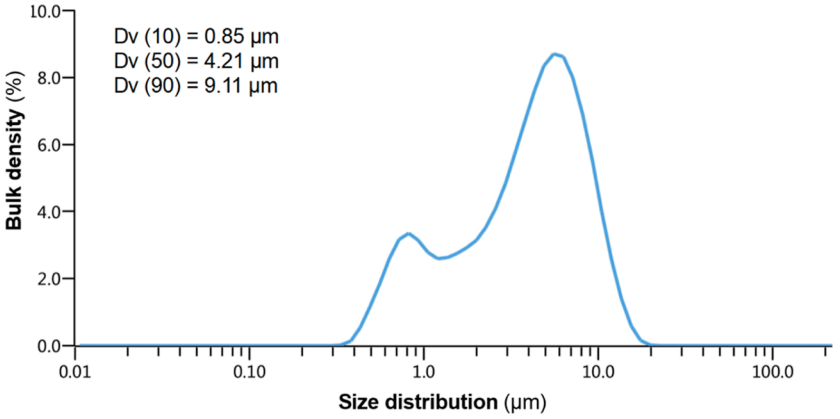

Figure 10. Particular size distribution of zeolite ZSM-5 synthesized from the mother liquor of 13X.

Table 3. BET Surface Area and Pore Characterization of Zeolites Produced from the FAAE Residue

	BET area (m^2/g)	V_{total} (cm^3/g)	V_{micro} (cm^3/g)[c]	V_{meso} (cm^3/g)[d]	pore size(nm)[e]
13X	444.8	0.1595[a]	0.1053	0.0473	1.4340
ZSM-5	384.2	0.1698[b]	0.1438	0.0348	1.3297

[a]Single-point adsorption total pore volume of pores less than 0.9384 nm in diameter at P/P_o = 0.0100. [b]Single-point adsorption total pore volume of pores less than 372.3423 nm^2 in diameter at P/P_o = 0.9943. [c]Total volume of the micropore by the *t*-plot model. [d]Adsorption cumulative volume of the mesopore calculated using the Barrett–Joyner–Halenda (BJH) model. [e]Adsorption average pore diameter by BET.

Table 4. Elemental Composition (by XRF, %) of the Zeolites Synthesized from the FAAE Residue[a]

	CO_2	Na_2O	K_2O	CaO	MgO	Al_2O_3	SiO_2	SAR
13X	3.50	18.77	0.017	0.011	0.02	32.31	44.87	2.36
ZSM-5	8.31	3.87	0.049	0.038	0.02	5.82	81.61	23.83
	P_2O_5	SO_3	Cl	TiO_2	Fe_2O_3	NiO	MoO_3	ZrO_2
13X	0.003	0.020	0.453	0.036	0.027	0.009	0.003	0.006
ZSM-5	bdl	0.017	0.066	bdl	0.134	bdl	0.009	bdl

[a]bdl, below the minimum detection limit.

production of 13X consumed a large amount of aluminum, which increased the silica/alumina ratio of the liquor to SAR = 32, suitable for the synthesis of ZSM-5.

Combined production of high-Si and low-Si zeolites maximized the utilization of both silicon and aluminum in the FAAE residue, reduced requirements for additional materials, and minimized the production of secondary waste. The strategies and practices developed in this study could be used to develop techniques for commercial disposal of fly ash in the future.

AUTHOR INFORMATION

Corresponding Author

Huidong Liu − *National Institute of Clean-and-Low-Carbon Energy, Beijing 102209, China*; orcid.org/0000-0002-8640-3956; Phone: +86 010-57336190; Email: 20022126@chnenergy.com.cn

Complete contact information is available at: https://pubs.acs.org/10.1021/acsomega.2c02388

https://doi.org/10.1021/acsomega.2c02388
ACS Omega 2022, 7, 20347−20356

Notes

The author declares no competing financial interest.

■ ACKNOWLEDGMENTS

This research was partially supported by the National Natural Science Foundation of China (grant number 42002196).

■ REFERENCES

(1) Luo, Y.; Wu, Y.; Ma, S.; Zheng, S.; Zhang, Y.; Chu, P. K. Utilization of coal fly ash in China: a mini-review on challenges and future directions. *Environ. Sci. Pollut. Res.* **2021**, *28*, 18727−18740.

(2) Xiao, Y. F.; Wang, B. D.; Liu, X. T.; Wang, X. H.; Zhao, L. J.; Yu, G. Z.; Sun, Q. Mechanism and kinetics study of sintering process for alumina recovery from fly ash. *Adv. Mater. Res.* **2014**, *955-959*, 2824−2830.

(3) Guo, Z.; Wei, C.; Zhang, P.; Han, J.; Chi, J.; Sun, Y.; Zhao, Y. Method for Preparing Metallurgical-Grade Alumina by Using Fluidized Bed Fly Ash. U.S. Patent 0,115,149 A1, 2013.

(4) Gao, Y.; Liang, K.; Gou, Y.; Wei, S. a.; Shen, W.; Cheng, F. Aluminum extraction technologies from high aluminum fly ash. *Rev. Chem. Eng.* **2021**, *37*, 885−906.

(5) Lei, Y.; Junzhou, C.; Yongwang, W.; Dong, C. Comprehensive utilization of alumina extraction from fly ash. *Clean Coal Technol.* **2014**, *20*, 113−115.

(6) Seredin, V. V.; Dai, S.; Sun, Y.; Chekryzhov, I. Y. Coal deposits as promising sources of rare metals for alternative power and energy-efficient technologies. *Appl. Geochem.* **2013**, *31*, 1−11.

(7) Dai, S.; Ren, D.; Li, S. Discovery of the superlarge gallium ore deposit in Jungar, Inner Mongolia, North China. *Chin. Sci. Bull.* **2006**, *51*, 2243−2252.

(8) Li, S.; Qin, S.; Kang, L.; Liu, J.; Wang, J.; Li, Y. An efficient approach for lithium and aluminum recovery from coal fly ash by pre-desilication and intensified acid leaching processes. *Metals* **2017**, *7*, 272.

(9) Dai, S.; Yan, X.; Ward, C. R.; Hower, J. C.; Zhao, L.; Wang, X.; Zhao, L.; Ren, D.; Finkelman, R. B. Valuable elements in Chinese coals: A review. *Int. Geol. Rev.* **2018**, *60*, 590−620.

(10) Ministry of Industry and Information Technology of China. Aluminium Industry Access Conditions. http://www.gov.cn/gzdt/2013-07/24/content_2454273.htm (accessed July 18, 2013).

(11) Yao, Z. T.; Xia, M. S.; Sarker, P. K.; Chen, T. A review of the alumina recovery from coal fly ash, with a focus in china. *Fuel* **2014**, *120*, 74−85.

(12) Sun, J. M.; Zhang, Z. J.; Chen, G.; Yan, S. Y.; Huo, Q. Z.; Wu, L. C.; Xu, H. L.; Qin, L.; Chen, X. X. Method for Co-Producing Alumina and Activated Calcium Silicate from High-Alumina Fly Ash. U.S. Patent 9,139,445 B2, 2015.

(13) Yadav, V. K.; Fulekar, M. H. Advances in methods for recovery of ferrous, alumina, and silica nanoparticles from fly ash waste. *Ceramics* **2020**, *3*, 384−420.

(14) Dang, G.; Han, Z.; Liu, J. Preparation of glass-ceramics from fly-ash residue after extraction valuable components. *Environ. Eng.* **2009**, *27*, 66−69.

(15) Wang, M.; Zheng, W.; Zhang, W.; Wang, W.; Chen, B.; Gao, Y. A method for preparing silicon carbide from pre-treated fly ash. CN 109607538 A, 2019.

(16) Wei, C.; Luo, F.; Jiang, Y.; Xue, B.; Sun, Y.; Li, F.; Gao, Q. Method for preparing rubber filler by modifying coal ash waste slag obtained after extracting aluminum through acid process. CN 102775816 B, 2012.

(17) Liu, P.; Zhang, Z.; Jia, M.; Gao, X.; Yu, J. ZSM-5 zeolites with different SiO2/Al2O3 ratios as fluid catalytic cracking catalyst additives for residue cracking. *Chin. J. Catal.* **2015**, *36*, 806−812.

(18) Rahimi, N.; Karimzadeh, R. Catalytic cracking of hydrocarbons over modified ZSM-5 zeolites to produce light olefins: A review. *Appl. Catal., A* **2011**, *398*, 1−17.

(19) Ramakrishna, D. V.; Jeeru, L. R.; Pradhan, N. C. Cracking of Heavy Oil over a Catalyst Synthesized from Fly Ash. In *Catalytic and Noncatalytic Upgrading of Oils*; Ajay, K. D., Dady, B. D., Zheng, Y., Duan, A., William, L. R., Sonil, N., Eds.; ACS Publication: New York, 2021; pp 211−231.

(20) Hamaguchi, T.; Tanaka, T.; Takahashi, N.; Tsukamoto, Y.; Takagi, N.; Shinjoh, H. Low-temperature no-adsorption properties of manganese oxide octahedral molecular sieves with different potassium content. *Appl. Catal., B* **2016**, *193*, 234−239.

(21) Zhang, K.; Van Dyk, L.; He, D.; Deng, J.; Liu, S.; Zhao, H. Synthesis of zeolite from fly ash and its adsorption of phosphorus in wastewater. *Green Process. Synth.* **2021**, *10*, 349−360.

(22) Watanabe, Y.; Yamada, H.; Kokusen, H.; Tanaka, J.; Moriyoshi, Y.; Komatsu, Y. Ion exchange behavior of natural zeolites in distilled water, hydrochloric acid, and ammonium chloride solution. *Sep. Sci. Technol.* **2003**, *38*, 1519−1532.

(23) Kobayashi, Y.; Ogata, F.; Saenjum, C.; Nakamura, T.; Kawasaki, N. Removal of Pb^{2+} from aqueous solutions using k-type zeolite synthesized from coal fly ash. *Water* **2020**, *12*, 2375.

(24) Ju, T.; Han, S.; Meng, Y.; Jiang, J. High-End Reclamation of Coal Fly Ash Focusing on Elemental Extraction and Synthesis of Porous Materials. *ACS Sustainable Chem. Eng.* **2021**, *9*, 6894−6911.

(25) Zhang, K.; Van Dyk, L.; He, D.; Deng, J.; Liu, S.; Zhao, H. Synthesis of zeolite from fly ash and its adsorption of phosphorus in wastewater. *Green Process. Synth.* **2021**, *10*, 349−360.

(26) Bandura, L.; Panek, R.; Madej, J.; Franus, W. Synthesis of zeolite-carbon composites using high-carbon fly ash and their adsorption abilities towards petroleum substances. *Fuel* **2021**, *283*, 119173.

(27) Iqbal, A.; Sattar, H.; Haider, R.; Munir, S. Synthesis and characterization of pure phase zeolite 4A from coal fly ash. *J. Cleaner Prod.* **2019**, *219*, 258−267.

(28) Ren, X.; Qu, R.; Liu, S.; Zhao, H.; Wu, W.; Song, H.; Zheng, C.; Wu, X.; Gao, X. Synthesis of zeolites from coal fly ash for the removal of harmful gaseous pollutants: A review. *Aerosol Air Qual. Res.* **2020**, *20*, 1127−1144.

(29) Chen, Y.; Cong, S.; Wang, Q.; Han, H.; Lu, J.; Kang, Y.; Kang, W.; Wang, H.; Han, S.; Song, H.; Zhang, J. Optimization of crystal growth of sub-micron ZSM-5 zeolite prepared by using $Al(OH)_3$ extracted from fly ash as an aluminum source. *J. Hazard. Mater.* **2018**, *349*, 18−26.

(30) Wang, X.; Wang, B.; Xiao, Y.; Liu, X.; Zhao, L.; Yu, G.; Sun, Q. Development of alumina & silica-based high valuable products from fly ash. *Annual International Pittsburgh Coal Conference*; Pittsburgh: Beijing, 2013.

(31) Liu, X. T.; Wang, B. D.; Yu, G. Z.; Xiao, Y. F.; Wang, X. W.; Zhao, L. J.; Sun, Q. Kinetics study of predesilication reaction for alumina recovery from alumina rich fly ash. *Mater. Res. Innovations* **2014**, *18*, 541−546.

(32) Tang, M.; Zhou, C.; Pan, J.; Zhang, N.; Liu, C.; Cao, S.; Hu, T.; Ji, W. Study on extraction of rare earth elements from coal fly ash through alkali fusion−Acid leaching. *Miner. Eng.* **2019**, *136*, 36−42.

(33) Zhou, B.; Zhou, J.; Hu, T.; Yang, L.; Lin, G.; Zhang, L. Phase transformation mechanism in activation of high-alumina fly ash with Na_2CO_3. *Mater. Res. Express* **2018**, *6*, 015502.

(34) Pan, J.; Hassas, B. V.; Rezaee, M.; Zhou, C.; Pisupati, S. V. Recovery of rare earth elements from coal fly ash through sequential chemical roasting, water leaching, and acid leaching processes. *J. Cleaner Prod.* **2021**, *284*, 124725.

(35) Aphane, M. E.; Doucet, F. J.; Kruger, R. A.; Petrik, L.; van der Merwe, E. M. Preparation of sodium silicate solutions and silica nanoparticles from South African coal fly ash. *Waste Biomass Valorization* **2020**, *11*, 4403−4417.

(36) Ma, Z.; Zhang, S.; Zhang, H.; Cheng, F. Novel extraction of valuable metals from circulating fluidized bed-derived high-alumina fly ash by acid−alkali−based alternate method. *J. Cleaner Prod.* **2019**, *230*, 302−313.

(37) Zeng, X.; Ye, Y.; Wang, M.; Qian, W.; Du, C. Synthesis of pure zeolites by dissolved silicon and aluminium from fly ash by stages (In Chinese). *Bull. Chin. Ceram. Soc.* **2007**, *26*, 19−24.

(38) Shoppert, A.; Valeev, D.; Loginova, I.; Chaikin, L. Complete Extraction of Amorphous Aluminosilicate from Coal Fly Ash by Alkali Leaching under Atmospheric Pressure. *Metals* **2020**, *10*, 1684.

https://doi.org/10.1021/acsomega.2c02388
ACS Omega 2022, 7, 20347−20356

(39) Liu, H.; Xiao, Y.; Jiang, X. Green Conversion of Coal Fly Ash into Soil Conditioner: Technological Principle and Process Development. *Minerals* **2022**, *12*, 276.
(40) Zong, Y.-b.; Zhao, C.-y.; Chen, W.-h.; Liu, Z.-b.; Cang, D.-q. Preparation of hydro-sodalite from fly ash using a hydrothermal method with a submolten salt system and study of the phase transition process. International Journal of Minerals. *Metall. Mater.* **2020**, *27*, 55−62.
(41) Bandarchian, F.; Anbia, M. Conventional hydrothermal synthesis of nanoporous molecular sieve 13X for selective adsorption of trace amount of hydrogen sulfide from mixture with propane. *J. Nat. Gas Sci. Eng.* **2015**, *26*, 1380−1387.
(42) Yuan, E.; Zhang, K.; Lu, G.; Mo, Z.; Tang, Z. Synthesis and application of metal-containing zsm-5 for the selective catalytic reduction of NOx with NH_3. *J. Ind. Eng. Chem.* **2016**, *42*, 142−148.
(43) Xue, T.; Chen, L.; Wang, Y. M.; He, M.-Y. Seed-induced synthesis of mesoporous zsm-5 aggregates using tetrapropylammonium hydroxide as single template. *Microporous Mesoporous Mater.* **2012**, *156*, 97−105.
(44) Zhao, X. Study on the synthesis technology of 13X (In Chinese). Master dissertation, Central South University, Changsha, China, 2005.
(45) Pourazar, M. B.; Mohammadi, T.; Jafari Nasr, M. R.; Javanbakht, M.; Bakhtiari, O. Preparation of 13x zeolite powder and membrane: investigation of synthesis parameters impacts using experimental design. *Mater. Res. Express* **2020**, *7*, 035004.
(46) Liu, Z.; Li, H.; Zhang, T.; Wang, Y.; Shi, P.; Wang, Y.; Subhan, F.; Liu, X.; Yan, Z. Mother liquor induced preparation of SAPO-34 zeolite for MTO reaction. *Catal. Today* **2020**, *358*, 109−115.
(47) Yang, J.; Huang, Y.-X.; Pan, Y.; Mi, J.-X. Green synthesis and characterization of zeolite silicalite-1 from recycled mother liquor. *Microporous Mesoporous Mater.* **2020**, *303*, 110247.
(48) Kumar, R.; Bhaumik, A.; Ahedi, R. K.; Ganapathy, S. Promoter-induced enhancement of the crystallization rate of zeolites and related molecular sieves. *Nature* **1996**, *381*, 298−300.
(49) Du, Y.; Lan, X.; Liu, S.; Ji, Y.; Zhang, Y.; Zhang, W.; Xiao, F. The search of promoters for silica condensation and rational synthesis of hydrothermally stable and well ordered mesoporous silica materials with high degree of silica condensation at conventional temperature. *Microporous Mesoporous Mater.* **2008**, *112*, 225−234.

https://doi.org/10.1021/acsomega.2c02388
ACS Omega 2022, 7, 20347−20356